

Cite this: *Dalton Trans.*, 2012, **41**, 644

www.rsc.org/dalton

PAPER

Diruthenium(II,III) tetramidates as a new class of oxygenation catalysts†

Leslie Villalobos, Zhi Cao, Phillip E. Fanwick and Tong Ren*

Received 27th May 2011, Accepted 26th September 2011

DOI: 10.1039/c1dt11530h

Two new diruthenium(II,III) tetramidate compounds, $\text{Ru}_2(\text{NHOCC}(\text{CH}_3)_2)_4\text{Cl}$ (**1**) and $\text{Ru}_2(\text{NHOCCH}_2\text{CH}_3)_4\text{Cl}$ (**2**) have been prepared and structurally characterized by X-ray crystallography. The activity of promoting sulfide oxygenation using simple oxidants such as hydrogen peroxide (H_2O_2) and *tert*-butyl hydroperoxide (TBHP) was studied. A UV-kinetics study indicated that the initial rates of **1** and **2** are comparable to the previously studied diruthenium tetracarboxylates in promoting TBHP oxygenation of methyl phenyl sulfide (MPS). Using excess oxidant and CH_3CN as the solvent, organic sulfides MPS and diphenyl sulfide (PPS) were oxidized using 1 mol% of the catalytic species. Compound **1** is more effective than **2** in converting sulfides to sulfoxide under the same conditions. Fast conversion was achieved when the reactions were carried out in the solvent-free conditions, and the major oxidation product was the sulfoxide. The electronic structure of the title compounds was studied with DFT calculations to gain an understanding of the activation of peroxy reagents.

Introduction

In recent years the synthetic modification of diruthenium tetracarboxylates with formula $[\text{Ru}_2(\text{O}_2\text{CR})_4\text{L}_2]^{0/+2+}$ by varying the groups R and L (R = alkyl and aryl, and L = Lewis base) has generated much interest.^{1–3} The ligand substitution reaction of $\text{Ru}_2(\text{OAc})_4\text{Cl}$ with amides results in the formation of diruthenium(II,III) tetramidate compounds of a paddlewheel framework as shown in Chart 1,^{4,5} where the triatomic (N–C–O) bridging ligands support the diruthenium core.

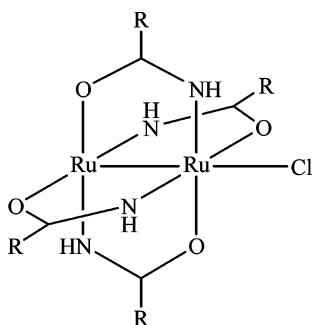


Chart 1 Diruthenium amidates of paddlewheel motif; R = isopropyl (**1**); R = ethyl (**2**).

Catalytic activities of $\text{Ru}_2(\text{II,III})$ tetracarboxylates have been reported for the hydrogenation of alkenes and alkynes,⁶ cyclo-

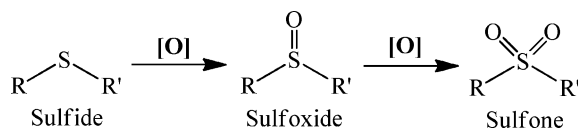
propanation and cross-metathesis of alkenes,⁷ and oxidation of organosulfur compounds.^{8,9} While the exact mechanism of the latter type reaction remains unknown, it is likely that the Ru_2 unit activates the peroxy species using one of its axial positions. Interesting examples of other diruthenium species as catalysts have been reported recently, including (i) the generation of transient axial Ru-nitrene and the isolation of the product of nitrene insertion into the aromatic CH bond by Berry,¹⁰ and (ii) olefin cyclopropanation with diazo agents catalyzed by diruthenium(I,I) mixed carbonyl carboxylate compounds.¹¹ Also noteworthy are the allylic and amine oxidations by *tert*-butyl hydroperoxide (TBHP) facilitated by various dirhodium catalysts.¹² Past studies on diruthenium tetramidates have addressed issues including synthetic methods, voltammetric and magnetic characterization, and electronic structures.^{4,13} The current study focuses on the influence of the amide ligands on the reactivity of the diruthenium center as peroxide activators for organic sulfide oxygenation. We are particularly interested in whether diruthenium tetramidates exhibit faster rates than $\text{Ru}_2(\text{esp})_2\text{Cl}$ ⁸ due to the enhanced electron richness of the Ru_2 core.¹⁴

The interest in the oxidation of organic sulfides originates from the utility of sulfoxides and sulfones in medicinal chemistry,¹⁵ the removal of refractory sulfur compounds from fossil fuels,¹⁶ and the decontamination of V type agents and mustard gas.^{17,18} Organosulfur compounds in fossil fuels are typically removed by hydrodesulfurization (HDS), biodesulfurization, and chlorine-based bleaching processes; these methods present certain drawbacks. For example, HDS technology requires extremely high temperatures and pressures, and the lowest sulfur content achieved is around 500 ppm because of its ineffectiveness in reducing DBT (dibenzothiophene) derivatives.¹⁹ The highest activity obtained using biodesulfurization is still insufficient to fulfil industrial

Department of Chemistry, Purdue University, 560 Oval Drive, West Lafayette, Indiana 47907, USA. E-mail: tren@purdue.edu

† Electronic supplementary information (ESI) available: Optimised model structures; electrochemical plots. CCDC reference numbers 827246–827247. For ESI and crystallographic data in CIF or other electronic format see DOI: 10.1039/c1dt11530h

requirements.²⁰ Processes used for the degradation and decontamination of chemical warfare agents, such as chlorine-based bleaching processes, are corrosive and can produce undesirable reaction byproducts that are harmful to the environment.¹⁷ A convenient and effective method to remove sulfur compounds from fossil fuels and to detoxify S-containing chemical warfare agents is sulfide oxygenation, where an organic sulfide is oxidized to its sulfoxide and then to its sulfone as presented in Scheme 1.²¹



Scheme 1 Oxygenation of organic sulfides.

Oxidants such as hydrogen peroxide and *tert*-butyl hydroperoxide are ideal, as they are environment-friendly reagents with water and *tert*-butyl alcohol as the respective by-products. The reactions between these oxidants and organic sulfides are slow; hence extensive studies have been performed for the development of new catalysts.²² Diruthenium catalysts such as $\text{Ru}_2(\text{OAc})_4\text{Cl}$ and $\text{Ru}_2(\text{esp})_2\text{Cl}$ ($\text{esp} = \alpha, \alpha', \alpha', \alpha'$ -tetramethyl-1,3-benzenedipropionic acid) have been successfully used to promote sulfide oxygenation by *tert*-butyl hydroperoxide in either an acetonitrile solution or neat (solvent-free) conditions.⁸ Considering the success of the diruthenium(II,III) tetracarboxylates in facilitating sulfide oxygenation, we wondered about the catalytic activity of more electron rich diruthenium species supported by amidate ligands. Reported herein are the synthesis of two new diruthenium(II,III) tetramidate compounds (Scheme 1) and their activity in promoting the oxygenation of methyl phenyl sulfide (MPS) and diphenyl sulfide (PPS), using hydrogen peroxide or *tert*-butyl hydroperoxide as the oxidant.

Results and discussion

A. Synthesis and characterization

Both compounds **1** and **2** were prepared by 24 h refluxing of $\text{Ru}_2(\text{OAc})_4\text{Cl}$ with 6 equiv. of the corresponding amide in toluene, which was outfitted with a micro-Soxhlet extraction apparatus containing $\text{K}_2\text{CO}_3/\text{sand}$ as the scrubber for acetic acid.²³ Recrystallization of compounds from hot methanol yielded brown crystalline materials. Similar to the previously studied diruthenium(II,III) tetramidates, compounds **1** and **2** are paramagnetic with room temperature effective magnetic moments of 3.6 and 3.8 μ_B , respectively, which correspond to a $S = 3/2$ ground state. The vis-NIR absorption spectra of both compounds **1** and **2** feature peaks at *ca.* 440 nm and 950 nm. The former is assigned to the $n(\text{Cl}) \rightarrow \pi^*(\text{Ru}_2)$ LMCT transition,²⁴ and the latter to $\delta(\text{Ru}_2) \rightarrow \delta^*(\text{Ru}_2)$ transition.²⁵ Redox properties of compounds **1** and **2** were examined with both cyclic (CV) and differential voltammetric (DPV) techniques in acetonitrile solutions (plots provided in the ESI†). Both compounds **1** and **2** exhibit quasi-reversible $1e^-$ oxidation at 0.53 V and 0.77 V *versus* Ag/AgCl , respectively. Despite the structural similarity between the two compounds, the formal potential of $1e^-$ oxidation of **1** is 0.24 V more cathodic than that of **2**, indicating that the former is significantly more electron rich than the latter. Quasi-reversible reductions were also

observed for both compounds and formal potential for **1** is more cathodic than that of **2**, further confirming the electron richness of **1**. It is worth noting that the oxidation of $\text{Ru}_2(\text{esp})_2\text{Cl}$ appears as an irreversible wave at *ca.* 0.84 V under the same conditions,²⁶ confirming that the tetramidates studied herein are more electron rich than diruthenium(II,III) tetracarboxylates.

Dinuclear paddlewheel compounds supported by *N,O*-bidentate bridging ligands may adopt one of four possible configuration isomers (Chart 2). The amidate ligand arrangement in each isomer may influence both the accessibility of axial sites and the electronic structure, and hence the structural details about compounds **1** and **2** are relevant to the oxygenation catalysis. Single crystals for both compounds were obtained by slow diffusion of ether into a saturated solution, and the molecular structures determined *via* single crystal X-ray diffraction are shown in Fig. 1.

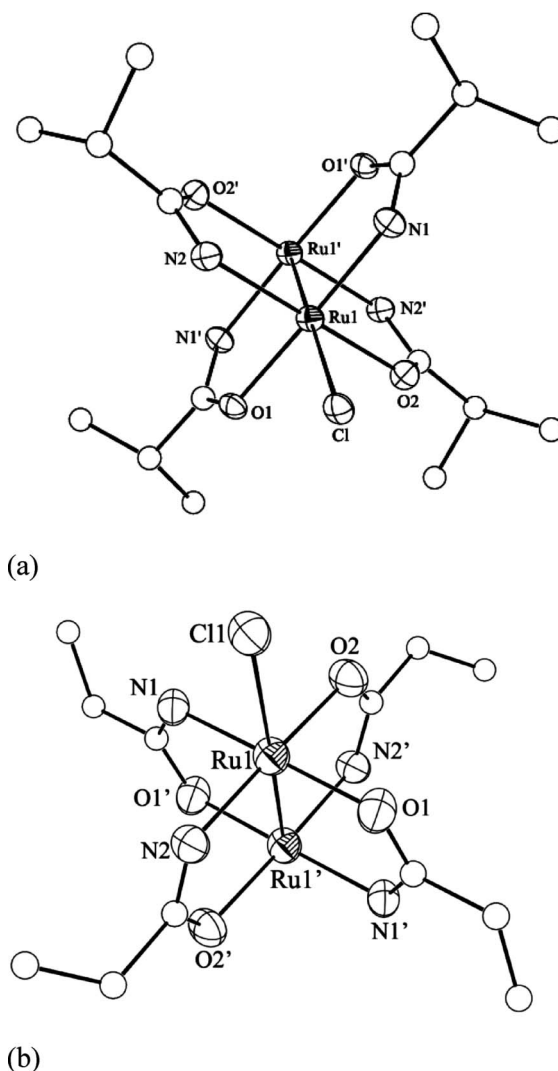


Fig. 1 Molecular structures of $\text{Ru}_2(\text{ONHCC}(\text{CH}_3)_2)_4\text{Cl}$ (**1**, a) and $\text{Ru}_2(\text{ONHC}(\text{CH}_2\text{CH}_2)_4)_4\text{Cl}$ (**2**, b). Hydrogen atoms were omitted for clarity and ellipsoids were plotted at 30% probability level.

It is clear from Fig. 1 that the amidate ligands adopt the *cis*-(2,2) arrangement similar to what has been previously reported for other diruthenium amidate compounds,²⁷ where the like atoms bound to the same Ru center are *cis* to each other. There is a crystallographic

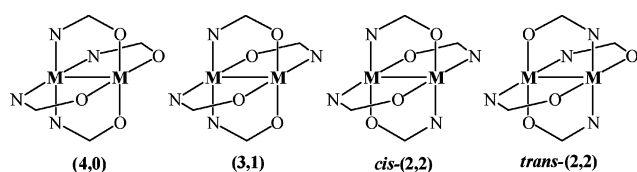


Chart 2 Configuration isomers in $M_2(N-O)_4$ type compounds.

Table 1 Selected bond lengths (Å) and angles (°) for compounds **1** and **2**

	1	2
Ru1–Ru1'	2.2997(7)	2.288(1)
Ru1–O1	2.067(3)	2.033(6)
Ru1–O2	2.050(3)	2.037(6)
Ru1–N1	2.033(4)	2.048(6)
Ru1–N2	2.026(4)	2.035(7)
Ru1–Cl	2.5671(9)	2.581(2)
Ru1'–Ru1–O1	91.9(1)	90.5(2)
Ru1'–Ru1–O2	91.51(9)	90.3(2)
Ru1'–Ru1–N1	86.9(1)	88.6(2)
Ru1'–Ru1–N2	87.2(1)	88.5(2)
Ru1–Ru1'–Cl	178.16(2)	177.7(5)

inversion center that bisects the Ru1–Ru1' bond in both cases. Furthermore, both compounds form one-dimensional zig-zag chain structures with axial Cl bridging the adjacent Ru_2 units, similar to many diruthenium(II,III) species supported by either carboxylate or amidate ligands.^{1,28} The Ru–Ru bond lengths in **1** and **2** are 2.2997(7) and 2.288(1) Å, respectively, which are comparable to the previously reported tetramidate compounds²⁷ and consistent with a formal bond order of 2.5. These distances are also similar to those found in analogous tetracarboxylates such as $Ru_2(O_2CCH_2CH_3)_4Cl$ with a Ru1–Ru1' distance equal to 2.292(7) Å.²⁹ Additional bond lengths and angles for compounds **1** and **2** are presented in Table 1.

To gain insight into the electronic structure of diruthenium tetramidates and the impact of H_2O_2 binding, spin-unrestricted DFT calculations were performed for both compound **1** and two hypothetical compounds $1' \cdot H_2O$ and $1' \cdot H_2O_2$, where the vacant axial position of **1** is occupied by a water and a hydrogen peroxide molecule, respectively. The geometry of model **1'** was fully optimized from the crystal structure of **1** at BP86/LanL2DZ level using the DFT method. The structures of $1' \cdot H_2O$ and $1' \cdot H_2O_2$ were constructed by the further full optimization of **1'** with a water molecule and a hydrogen peroxide molecule added to the five-coordinated Ru center, respectively. The bond lengths and angles around the Ru_2 core in the optimized geometry of **1** match well with those from the crystal structure, and the optimized geometries for all three model compounds are given in the ESI.† Fig. 2 shows the computed frontier molecular orbital diagrams for compounds **1'**, $1' \cdot H_2O$, and $1' \cdot H_2O_2$.

Calculations for both model compounds **1'** and $1' \cdot H_2O$ converged to similar configurations with SOMO, SOMO–1, and SOMO–2 being singly occupied. It is clear from Fig. 2 that the SOMOs in both cases are predominantly the $\delta^*(Ru-Ru)$ orbital with an additional contribution from the lone pairs of N and O centers of the amidate ligands. The SOMO–1 and SOMO–2 are nearly degenerate with a separation of 0.029 and 0.025 eV in **1'** and $1' \cdot H_2O$, respectively. They are primarily the $\pi^*(Ru-Ru)$ orbitals with significant contribution from the $p(Cl)$ lone pair. The LUMO

of **1** is predominantly a $\sigma^*(Ru-Ru)$ orbital, as noted in the previous studies of similar compounds.^{3,30} Of special notice is the electron density (d_{z^2}) stacked along the axial direction at the unsaturated 5-coordinated Ru center in the LUMO. Upon the introduction of the H_2O molecule (namely $1' \cdot H_2O$), the stacked d_{z^2} electron density partially shifts to the H_2O , leading to a more relaxed Ru–Ru bond distance, 2.375 Å (2.355 Å in **1'**). The addition of the axial H_2O seems to destabilize all Ru_2 based MOs when compared with those of **1'** and the LUMO being the most destabilized. The coordination to Ru_2 also brought subtle changes in H_2O : the O–H bond elongated from 0.975 Å in free H_2O to 0.977 Å, and the H–O–H angle relaxed from 104.5 to 112.1 degree. The latter reflects the conversion of one of the H_2O 's lone pairs into a dative bonding pair. One may infer from the DFT result of $1' \cdot H_2O$ that the electron density along the Ru–Ru axial position would be imparted onto H_2O_2 upon its coordination, which leads to weakened Ru–Ru and O–O bonds. The latter would lead to the activation of the peroxy species.

The preceding conjecture was verified with the DFT study of $1' \cdot H_2O_2$. Similar to the cases of **1'** and $1' \cdot H_2O$, the calculation of $1' \cdot H_2O_2$ converged to a configuration with SOMO, SOMO–1, and SOMO–2 being singly occupied, and the compositions of these SOMOs are comparable across the series as shown in Fig. 2. Clearly, the presence and nature of the dative ligand (H_2O or H_2O_2) has a minimal impact on the electronic structure of the Ru_2 core. There is a slight lengthening of Ru–Ru bond in $1' \cdot H_2O_2$ (2.388 Å) in comparison with that of $1' \cdot H_2O$ (2.375 Å). On the other hand, the O–O bond in $1' \cdot H_2O_2$ has been significantly elongated to 1.618 Å from that of free H_2O_2 (1.475 Å).³¹ This result points to the pivotal role of the dative coordination of peroxy species to Ru_2 in the eventual O–O bond cleavage.

B. Oxygenation catalysis

Successful preparation and characterization of **1** and **2** was followed by the examination of their ability in facilitating the oxygenation of methyl phenyl sulfide (MPS) and phenyl sulfide (PPS) using H_2O_2 and TBHP as the oxidants in CH_3CN . The data obtained through GC analysis are presented in Tables 2 and 3 for oxidants as H_2O_2 and TBHP, respectively. As shown in Table 2, compounds **1** and **2** are active for the oxygenation of MPS and PPS. The highest rate of conversion was obtained for the MPS oxidation using **1**: MPS was completely consumed in 24 h to yield 71% MPSP and 27% MPSP₂. Oxygenation of PPS is slower than that of MPS and a significant amount of sulfide was still present at 24 h with **1** (entry 6) under the same conditions as that for MPS (entry 3). It is clear from comparing the turn-over-frequencies (TOFs) of entries 3 and 9 that catalyst **2** is slightly less efficient than **1**. Previously, we reported TOFs as high as 5000 for organic sulfide oxygenation by H_2O_2 with Mn–Me₃TACN catalysts.³² Clearly, the diruthenium tetramidate catalysts **1** and **2** are inferior in terms of reaction rate. However, the amide ligands are much less expensive than Me₃TACN, which make **1** and **2** suitable candidates when the rate is not the crucial factor in the selection of catalysts.

The proficiency of compounds **1** and **2** in facilitating TBHP oxygenation was similarly examined and the results are given in Table 3. It is clear from Table 3 (entries 13–24) that both **1** and **2** are capable of activating TBHP, with **1** being slightly faster than **2**. Furthermore, the reactions using TBHP are universally slower

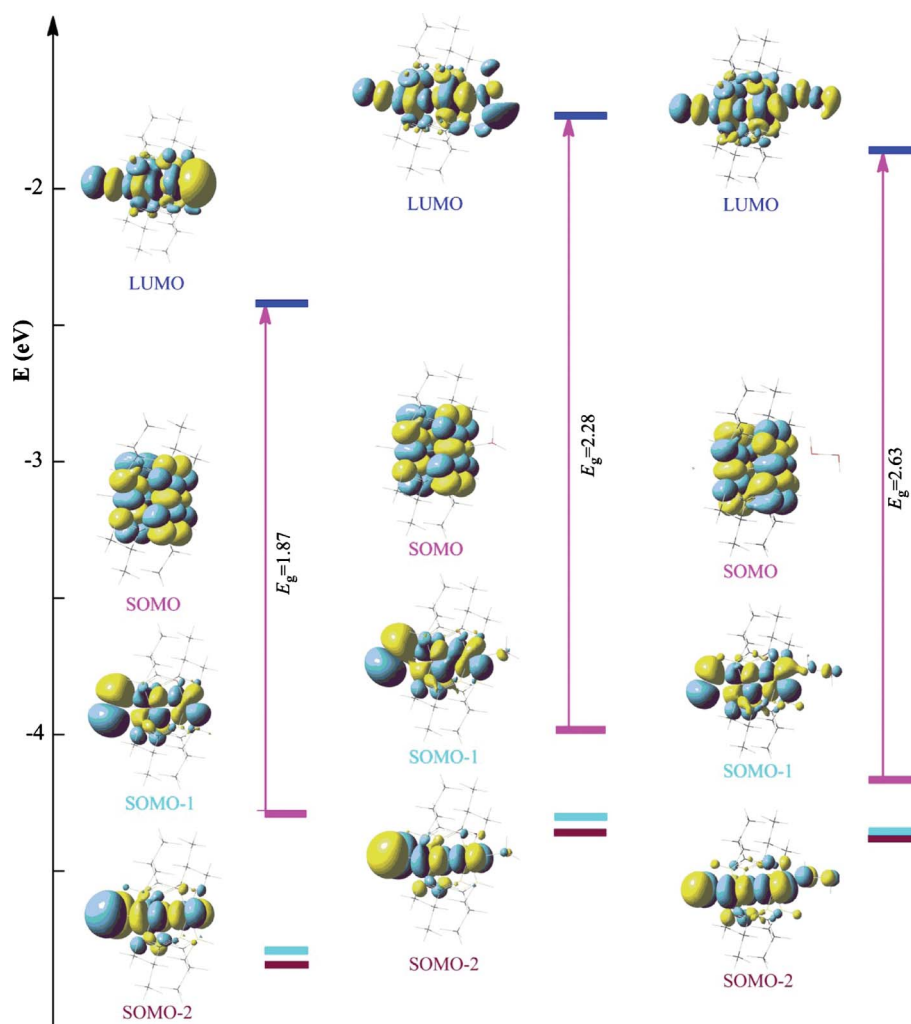


Fig. 2 Molecular orbital diagram model compounds **1'** (left), **1'**-H₂O (middle) and **1'**-H₂O₂ (right) obtained from DFT calculations.

Table 2 Results for the analysis of MPS and PPS oxidation using 1 mol % of catalyst and 8 equiv. of H₂O₂^a

Catalyst	RSR'	Entry	<i>t</i> /h	RSR ^a %	RSOR ^a %	RSO ₂ R ^a %	TOF ^b
1	MPS	1	2	19	73	6	43
		2	6	5	81	14	18
		3	24	0	71	27	5.2
	PPS	4	2	62	33	4	21
		5	6	48	45	6	10
		6	24	38	51	9	2.9
2	MPS	7	2	28	71	2	38
		8	6	12	82	5	15
		9	24	1	89	10	4.5
	PPS	10	2	64	34	2	19
		11	6	51	43	4	9
		12	24	37	56	7	2.9

^a Reaction conditions: 10 mL of solvent, 0.5 mmol of substrate, 4 mol H₂O₂, 0.005 mmol of catalyst; room temperature. ^b Turn-over-frequency (hour⁻¹) = {[RR'SO] + 2[RR'SO₂]} / {[Cat]**t* (h)}.

than the corresponding reactions using H₂O₂. The comparison of catalytic efficiency of **1** and **2** with that of Ru₂(esp)₂Cl is interesting and perplexing. While both **1** and **2** (entries 13 and 19) are comparable to Ru₂(esp)₂Cl in terms of TOF of MPS oxygenation

during the early phase of the reactions, they did not result in the complete consumption of MPS at 24 h (entries 15 and 21) as did Ru₂(esp)₂Cl.⁸ Initial rate studies based on UV spectroscopic techniques were performed to address this issue as described below. It was found in the early study of Ru₂(esp)₂Cl that the solubility of the catalyst in non-polar solvents allows solvent free reaction conditions.⁸ The same type of solvent free catalytic reactions were performed by dissolving either **1** or **2** directly into organic sulfide and initiating the reactions by the addition of TBHP. As seen on entries 25 and 27, the TOFs of MPS oxygenation were drastically enhanced compared to those obtained in CH₃CN (entries 13 and 19). Nevertheless, these results are not nearly as good as those from using Ru₂(esp)₂Cl, where nearly quantitative conversion of MPS to MPSO was achieved with only one equiv. of TBHP.⁸

To better understand the less than desired performance of compounds **1** and **2** as oxygenation catalysts, the initial rates of MPS oxygenation reactions were investigated using UV absorption spectroscopy. The consumption of MPS can be monitored by the disappearance of the band at 290 nm (*n*(S) → *π**(ph)) as described in prior studies.^{8,33} The dependence of reaction rates on both [**1**] and [**2**] was monitored for the first 30 min under pseudo first order conditions (100 equiv. TBHP) and the initial rates (*k*_{obs}) were extracted from the natural logarithm of the

Table 3 TBHP oxygenation of organic sulfides

Catalyst	RSR'	Entry	t/h	RSR' %	RSOR' %	RSO ₂ R' %	TOF
1	MPS	13	2	40	52	5	31
		14	6	39	54	5	11
		15	24	26	69	5	3
	PPS	16	2	78	16	4	12
		17	6	75	19	5	5
		18	24	70	24	6	1.5
2	MPS	19	2	59	35	5	23
		20	4	54	38	6	13
		21	24	40	54	6	3
	PPS	22	2	77	16	2	10
		23	6	73	22	3	5
		24	24	51	34	12	2
<i>Solvent free conditions^b</i>							
1	MPS	25	1	0	90	9	108
	PPS	26	1	58	40	0	40
2	MPS	27	1	2	84	14	112
	PPS	28	1	64	36	0	36
<i>Catalyst stability test^c</i>							
1	MPS	29	1.5	5	62	31	83
		30	24	5	60	35	5

Conditions:^a (top half) 0.5 mmol of substrate, 4 mmol TBHP, 0.005 mmol of catalyst, 10 mL of solvent; room temperature ^b Solvent free: 0.5 mmol of substrate, 4 mmol TBHP, 0.005 mmol of catalyst; room temperature. ^c Catalyst stability test: 0.5 mmol of substrate, 50 mmol TBHP, 0.005 mmol of catalyst; room temperature.

absorbance values plotted *versus* time. The initial rates plotted *versus* catalyst concentration are shown in Fig. 3 for compounds **1**, **2** and Ru₂(esp)₂Cl, from which the pseudo first order rate constant k' was obtained.

$$k_{\text{obs}} = k'[\text{cat}] \quad (1)$$

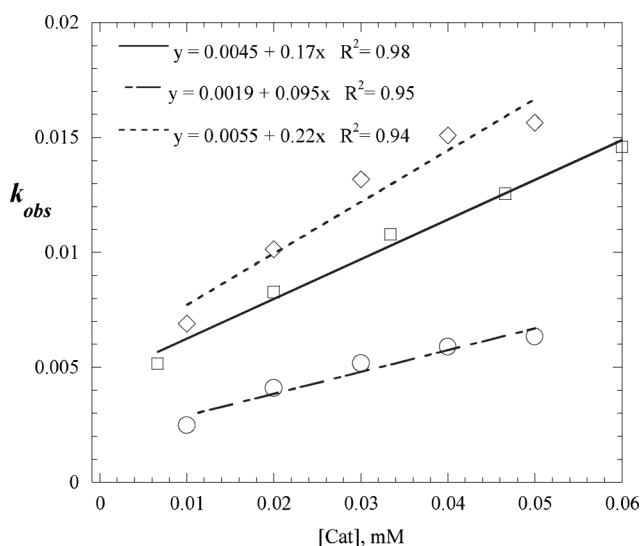


Fig. 3 Dependence of k_{obs} on **[1]** (diamond), **[2]** (circle) and **[Ru₂(esp)₂Cl]** (square) in MeCN in the oxygenation of MPS using TBHP.

The k' values obtained for **1** and **2** are 0.22 and 0.095 min⁻¹, respectively, and the former is comparable to that found for Ru₂(esp)₂Cl (0.17 min⁻¹) under the same conditions.⁸ While the k' values of **1** and **2** would predict similar catalytic efficiency to Ru₂(esp)₂Cl, their sluggish performance implies that some other limiting factors, such as the stability of the catalysts, affect the

course of catalytic reactions. Indeed, when MPS oxygenation was performed using 100 equiv. of TBHP (entries 29 and 30), significant conversion of MPS was achieved during the first 1.5 h but little reactivity was detected thereafter (1.5–24 h), suggesting that the majority of the catalyst was degraded during the first 1.5 h. Furthermore, the reaction mixture with **1** or **2** generally changes from an initial yellow color to a persistent dark purple during the course of the catalytic reaction with TBHP. Upon the reaction with 8 equiv. of TBHP in the absence of organic sulfide, both catalysts **1** and **2** were converted to dark purple species that are spectroscopically distinct from the pristine catalysts (see Fig. S1 and S2 in the ESI for spectral comparison†). Similar changes were observed with H₂O₂ as the oxidant.

Conclusion

Two new diruthenium tetramidate compounds (**1** and **2**) were synthesized and characterized with spectroscopic, voltammetric techniques and theoretical calculations. The ability of both **1** and **2** in promoting oxygenation of organic sulfides using H₂O₂ and TBHP at ambient conditions has been demonstrated. Diruthenium tetramidates are less active than the previously studied diruthenium tetracarboxylates. It appears that the enhanced electron richness actually led to faster degradation of the catalysts. Currently, we are investigating the feasibility of the other extreme—maintaining catalytic activity while increasing the longevity by using more electron deficient Ru₂ species.

Experimental

General considerations

MPS, PPS and the internal standard 1,2-dichlorobenzene were purchased from ACROS Organics. The ligands, isobutyramide and propionamide, were purchased from Sigma–Aldrich, the 30% H₂O₂ from Mallinkroft Chemicals and the 70% *tert*-butyl hydroperoxide also from ACROS Organics. All reagents were used as received. Ru₂(AcO)₄Cl was prepared as described in the literature.³⁴ Spectroscopic absorption spectra were collected with a JASCO V-670 spectrophotometer. The GC data were recorded on an Agilent 7890A Gas Chromatographic equipped with a HP-5 capillary column. Infrared spectra were recorded using a JASCOFT/IR-ATR 6300 spectrometer. All HR-nESI-MS data were performed on a modified QqTOF tandem mass spectrometer in CH₂Cl₂ (QSTAR XL; mass resolving power ~8000 amu; mass accuracy ~20 ppm; Applied Biosystems/MDS Sciex, Concord, ON, Canada). Masses were calculated by isotopic distribution utilizing Analyst 1.4 software (Applied Biosystems/MDS Sciex, Concord, ON, Canada). Both cyclic voltammetry (CV) and differential pulse voltammetry (DPV) were performed on a CHI620A voltammetric analyzer with a glassy-carbon working electrode (diameter 2 mm), a Pt-wire auxiliary electrode, and a Ag/AgCl reference electrode. All the reactions reported were carried out at room temperature and environmental pressure unless otherwise specified.

Ru₂(HNOC(CH₃)₂)₂Cl (**1**)

A mixture of Ru₂(OAc)₄Cl (475 mg, 1 mmol) and isobutyramide (522 mg, 6 mmol) was suspended in 60 mL of toluene and refluxed

with a condenser outfitted by a Soxhlet extraction apparatus containing K_2CO_3 for approximately 24 h. After the solvent removal, the residue was dissolved in hot methanol, filtered and recrystallized by the addition of ether. Compound **1** was isolated as an orange-brown microcrystalline material (0.401 g, 62%). Data for **1**: HR-nESI-MS based on ^{101}Ru , m/z 547.053, corresponding to $[M-Cl]^+$ (calc. 547.057). UV-Vis-NIR, λ_{max} (nm, ϵ ($M^{-1} cm^{-1}$)): 335(4490), 465(960), 999(200); IR (cm^{-1}) N–H 3299(m), 3351(m), C=O 1637(m), C–N 1442(m). Cyclic voltammogram [$E_{1/2}/V$, $\Delta E_p/V$, $i_{backward}/i_{forward}$]: 0.562, 0.038, 0.70. μ_{eff} : 3.56 μ_B .

Ru₂(HNOC(CH₂CH₃))₄Cl (2**)**

A mixture of Ru₂(OAc)₄Cl (475 mg, 1 mmol) and propionamide (430 mg, 6 mmol) was dissolved in 60 mL of toluene and refluxed as described above for 24 h. The color of the mixture changed from red-purple to dark brown. Compound **2** was recrystallized as described for compound **1** and isolated as dark brown microcrystalline material (0.573, 73%). Data for **2**: HR-nESI-MS based on ^{101}Ru , m/z 486.959, corresponding to $[M-Cl]$ (486.960). UV-Vis-NIR, λ_{max} (nm, ϵ ($M^{-1} cm^{-1}$)): 341(3260), 467(1090), 1014(150); IR (cm^{-1}) N–H 3318(m), 3342(m), C=O 1635(m), C–N 1436(m). Cyclic voltammogram [$E_{1/2}/V$, $\Delta E_p/V$, $i_{backward}/i_{forward}$]: 0.862, 0.094, 0.60. μ_{eff} : 3.83 μ_B .

Crystal structure determination

Single crystals suitable for X-ray diffraction were isolated *via* slow diffusion of ether into a saturated methanol solution. For the determination of the crystal structure, a brown needle of compound **1** having approximate dimensions of 0.16 × 0.08 × 0.05 mm and an orange needle of **2** having approximate dimensions of 0.16 × 0.04 × 0.01 mm were mounted on a fiber in a random orientation. Diffraction data was collected on a Rigaku Rapid II diffractometer using Cu-K α at 150(1) K and Frames were integrated with DENZO-SMN.³⁵ The structures were solved by direct methods using SIR2004,³⁶ and refinement was performed using SHELX-97.³⁷ Crystallographic data for **1** and **2** is presented in Table 4.

Computational details

Theoretical calculations were performed on model compounds **1'**, **1'**·H₂O and **1'**·H₂O₂ with Gaussian 03. Geometry optimizations

were performed with the generalized gradient approximation, using Becke's non-local correction to exchange and Perdew's non-local correction to correlation (BP86).³⁸ The basis set used was the LanL2DZ effective core potential³⁹ for the metal centers and 6-31G(d,p) for the ligand atoms. No negative frequency was observed in the vibrational frequency analysis.

Catalytic runs

For all the reactions presented, 2.5 mmol of the organic sulfide was placed in a flask with 2.0 mmol of the internal standard (1,2-dichlorobenzene) and 0.025 mmol of the catalyst and dissolved in 10 mL of MeCN. Solvent free reactions were done by dissolving the catalyst directly into the organic sulfide. Reactions were started by the addition of the corresponding amount of 9.7 M H₂O₂ solution or 7.6 M TBHP solution. Oxidant solution concentrations were determined by iodometric analysis. Results for entries 1–30 are an average of two runs. The turn-over-frequencies (TOF h^{−1}) were calculated using the equation $([RSOR'] + 2[RSO_2R'])/(1 \times t \text{ (h)})$.

Kinetic studies

UV experiments to measure the effects of catalyst concentration on the MPS oxidation was studied in a pseudo first order environment by using an excess of TBHP (100 equiv. in relation to MPS). Reaction rates were calculated when using 1, 2, 4 and 5 mol % of catalyst. Results were collected by monitoring the disappearance of the UV absorption band at 290 nm as previously reported.⁴⁰ Further details are given in the Results and discussion section.

Acknowledgements

This work was supported by both the US Army Research Office (Grant W911NF-06-1-0305) and Purdue University. We thank Mr. Yang Gao for his assistance in acquiring HR-MS data.

References

- P. Angaridis, *Ruthenium Compounds*, in: *Multiple Bonds between Metal Atoms*, ed. F. A. Cotton, C. A. Murillo and R. A. Walton, Springer Science and Business Media, Inc, New York, 2005; M. A. S. Aquino, *Coord. Chem. Rev.*, 2004, **248**, 1025.
- R. Gracia, H. Adams and N. J. Patmore, *Dalton Trans.*, 2009, 259; R. Gracia, H. Adams and N. J. Patmore, *Inorg. Chim. Acta*, 2010, **363**, 3856; D. A. Boyd, R. J. Crutchley, P. E. Fanwick and T. Ren, *Inorg. Chem.*, 2010, **49**, 1322.
- D. A. Boyd, Z. Cao, Y. Song, T.-W. Wang, P. E. Fanwick, R. J. Crutchley and T. Ren, *Inorg. Chem.*, 2010, **49**, 11525.
- M. Y. Chavan, F. N. Feldmann, X. Q. Lin, J. L. Bear and K. M. Kadish, *Inorg. Chem.*, 1984, **23**, 2373; A. R. Chakravarty, F. A. Cotton and D. A. Tocher, *Polyhedron*, 1985, **4**, 1097.
- A. R. Chakravarty and F. A. Cotton, *Polyhedron*, 1985, **4**, 1957; M. C. Barral, R. Jimenezaparcio, C. Rial, E. Royer, M. J. Saucedo and F. A. Urbanos, *Polyhedron*, 1990, **9**, 1723.
- P. Legzdins, R. W. Mitchell, G. L. Rempel, J. D. Ruddick and G. Wilkinson, *J. Chem. Soc. A*, 1970, 3322.
- A. F. Noels, A. Demonceau, E. Carlier, A. J. Hubert, R. L. Marquezsilva and R. A. Sanchezdelgado, *J. Chem. Soc., Chem. Commun.*, 1988, 783.
- J. E. Barker and T. Ren, *Inorg. Chem.*, 2008, **47**, 2264.
- H. B. Lee and T. Ren, *Inorg. Chim. Acta*, 2009, **362**, 1467.
- A. K. M. Long, R. P. Yu, G. H. Timmer and J. F. Berry, *J. Am. Chem. Soc.*, 2010, **132**, 1228; A. K. M. Long, G. H. Timmer, J. S. Pap, J. L. Snyder, R. P. Yu and J. F. Berry, *J. Am. Chem. Soc.*, 2011, **133**, 13138.
- Y. Sevryugina, B. Weaver, J. Hansen, J. Thompson, H. M. L. Davies and M. A. Petrukhina, *Organometallics*, 2008, **28**, 1750; B. Saha, T.

Table 4 Crystallographic data for compounds **1** and **2**

	1 ·2CH ₃ OH	2
Formula	C ₁₈ H ₄₀ ClN ₄ O ₆ Ru ₂	C ₁₂ H ₂₀ ClN ₄ O ₄ Ru ₂
Formula weight	646.14	521.91
Space group	P2/c (No. 13)	C2/c (No. 15)
a/Å	11.6827(8)	10.436(1)
b/Å	9.4837(5)	12.864(1)
c/Å	12.5641(9)	12.657(2)
$\beta/^\circ$	101.481(7)	93.192(4)
$V/\text{\AA}^3$	1364.2(2)	1696.6(4)
Z	2	4
$\rho_c/g\text{ cm}^{-3}$	1.573	2.043
T/K	150	150
Data collected	5761	5703
Unique data (R_{int})	2357 (0.057)	1403 (0.043)
$R_1(\text{obs})$, $wR_2(\text{obs})$	0.047, 0.135	0.061, 0.182

- Ghatak, A. Sinha, S. M. W. Rahaman and J. K. Bera, *Organometallics*, 2011, **30**, 2051.
- 12 M. O. Ratnikov, L. E. Farkas, E. C. McLaughlin, G. Chiou, H. Choi, S. H. El-Khalafy and M. P. Doyle, *J. Org. Chem.*, 2011, **76**, 2585; E. C. McLaughlin, H. Choi, K. Wang, G. Chiou and M. P. Doyle, *J. Org. Chem.*, 2009, **74**, 730; E. C. McLaughlin and M. P. Doyle, *J. Org. Chem.*, 2008, **73**, 4317; H. Choi and M. P. Doyle, *Chem. Commun.*, 2007, 745; A. J. Catino, J. M. Nichols, H. Choi, S. Gottipamula and M. P. Doyle, *Org. Lett.*, 2005, **7**, 5167.
 - 13 T. Malinski, D. Chang, F. N. Feldmann, J. L. Bear and K. M. Kadish, *Inorg. Chem.*, 1983, **22**, 3225; M. C. Barral, I. de la Fuente, R. Jimenez-Aparicio, J. L. Priego, M. R. Torres and F. A. Urbanos, *Polyhedron*, 2001, **20**, 2537.
 - 14 Oxygenation of organic sulfides may proceed *via* one of two major pathways, nucleophilic or electrophilic attack at the *S* center. An electron rich catalyst may promote the former.
 - 15 I. Fernandez and N. Khair, *Chem. Rev.*, 2003, **103**, 3651.
 - 16 A. Stanislaus, A. Marafi and M. S. Rana, *Catal. Today*, 2010, **153**, 1.
 - 17 B. M. Smith, *Chem. Soc. Rev.*, 2008, **37**, 470.
 - 18 S. S. Talmage, A. P. Watson, V. Hauschild, N. B. Munro and J. King, *Curr. Org. Chem.*, 2007, **11**, 285.
 - 19 I. V. Babich and J. A. Moulijn, *Fuel*, 2003, **82**, 607.
 - 20 M. Soleimani, A. Bassi and A. Margaritis, *Biotechnol. Adv.*, 2007, **25**, 570.
 - 21 Y. C. Yang, J. A. Baker and J. R. Ward, *Chem. Rev.*, 1992, **92**, 1729; A. R. Supale and G. S. Gokavi, *Catal. Lett.*, 2008, **124**, 284.
 - 22 J.-E. Backvall, *Selective Oxidation of Amines and Sulfides*, in: *Modern Oxidation Methods*, ed. J.-E. Backvall, Wiley-VCH, 2010.
 - 23 M. P. Doyle, V. Bagheri, T. J. Wandless, N. K. Harn, D. A. Brinker, C. T. Eagle and K. L. Loh, *J. Am. Chem. Soc.*, 1990, **112**, 1906; M. P. Doyle, W. R. Winchester, J. A. A. Hoorn, V. Lynch, S. H. Simonsen and R. Ghosh, *J. Am. Chem. Soc.*, 1993, **115**, 9968; G. Zou, J. C. Alvarez and T. Ren, *J. Organomet. Chem.*, 2000, **596**, 152.
 - 24 M. C. Barral, R. Jimenezaparcio, J. L. Priego, E. C. Royer, F. A. Urbanos, A. Monge and C. Ruizvalero, *Polyhedron*, 1993, **12**, 2947.
 - 25 V. M. Miskowski and H. B. Gray, *Inorg. Chem.*, 1988, **27**, 2501; V. M. Miskowski, T. M. Loehr and H. B. Gray, *Inorg. Chem.*, 1987, **26**, 1098.
 - 26 J. E. Barker, PhD thesis, University of Miami, 2006.
 - 27 A. R. Chakravarty and F. A. Cotton, *Polyhedron*, 1985, **4**, 1957.
 - 28 M. J. Bennett, K. G. Caulton and F. A. Cotton, *Inorg. Chem.*, 1969, **8**, 1.
 - 29 A. Bino, F. A. Cotton and T. R. Felthouse, *Inorg. Chem.*, 1979, **18**, 2599.
 - 30 L. Zhang, B. Xi, I. P. C. Liu, M. M. R. Choudhuri, R. J. Crutchley, J. B. Updegraff, J. D. Protasiewicz and T. Ren, *Inorg. Chem.*, 2009, **48**, 5187.
 - 31 B. F. Pedersen, *Acta Crystallogr., Sect. B: Struct. Crystallogr. Cryst. Chem.*, 1972, **28**, 1014.
 - 32 J. E. Barker and T. Ren, *Tetrahedron Lett.*, 2004, **45**, 4681.
 - 33 T. S. Smith and V. L. Pecoraro, *Inorg. Chem.*, 2002, **41**, 6754.
 - 34 T. Stephens and G. Wilkinson, *J. Inorg. Nucl. Chem.*, 1966, **28**, 2285.
 - 35 Z. Otwinowski and W. Minor, *Methods Enzymol.*, 1997, **276**, 307.
 - 36 M. C. Burla, R. Caliendo, M. Camalli, B. Carrozzini, G. L. Cascarano, L. De Caro, C. Giacovazzo, G. Polidori and R. Spagna, *J. Appl. Crystallogr.*, 2005, **38**, 381.
 - 37 G. M. Sheldrick, *Acta Crystallogr., Sect. A: Found. Crystallogr.*, 2008, **64**, 112.
 - 38 A. D. Becke, *Phys. Rev. A: At., Mol., Opt. Phys.*, 1988, **38**, 3098; J. P. Perdew, *Phys. Rev. B*, 1986, **33**, 8822.
 - 39 W. R. Wadt and P. J. Hay, *J. Chem. Phys.*, 1985, **82**, 284.
 - 40 K. A. Vassell and J. H. Espenson, *Inorg. Chem.*, 1994, **33**, 5491.